

Technical note

Effect of abrasive grinding on the strength of Y-TZP

Chang-Ju Ho, Hsuan-Chih Liu, Wei-Hsing Tuan*

Department of Materials Science & Engineering, National Taiwan University, Taipei 106, Taiwan

Received 20 August 2008; received in revised form 9 February 2009; accepted 23 February 2009

Available online 20 March 2009

Abstract

The residual stress and flaw size in yttria-stabilized zirconia (Y-TZP) before and after abrasive grinding are examined in the present study. As long as the distribution of flaw size remains the same after grinding, the strength of zirconia increases with increasing residual stress. For the grinding conditions employed, a compressive residual stress as high as 1 GPa is introduced on the surface. Such stress is large enough to induce lattice distortion. The strength of Y-TZP is consequently increased by 190 MPa. The compressive residual stress can be partly removed by subsequent polishing or annealing treatment.

© 2009 Elsevier Ltd. All rights reserved.

Keywords: ZrO₂; Grinding; Residual stress; Strength

1. Introduction

Yttria-stabilized zirconia (Y-TZP) has received great interest for engineering applications due to its superb mechanical performance.^{1,2} For many structural applications, dimensional tolerance has to be tightly controlled. Abrasive grinding is therefore frequently used to meet such requirement. During abrasive grinding, material together with the flaws in the surface region are removed, while residual stresses are introduced into the newly formed surface region. The magnitude of the residual stresses can be determined by using several techniques.^{3–8} Typically, these techniques reveal only the residual stress at the surface region.

As zirconia is used as all-ceramic crowns or fixed partial dentures, a polishing treatment is frequently conducted after grinding to obtain a cosmetic effect. A polishing treatment can remove the residual stress induced by prior grinding.⁶ However, depending on the polishing details, some polishing techniques may even induce residual stress in the surface region.⁸

The residual stress induced by abrasive grinding is compressive on the surface and tensile underneath.⁶ The reported values on the magnitude of residual stress differ significantly from one report to another one. The difference may be resulted partly from different measurement techniques, partly from different grind-

ing conditions. For example, a dressing treatment on diamond wheel prior grinding increased significantly the residual stress in a silicon nitride.⁸ The contribution of the residual stress to the strength of the ground specimens is not clear. For example, some studies indicated that the strength and Weibull modulus of an alumina were increased after abrasive grinding⁹; however, some studies demonstrated that the strength and Weibull modulus of a zirconia were decreased after grinding.^{10,11}

The residual stress can be reduced by applying an annealing treatment.⁹ However, the size of flaws may be changed during annealing. Since the change of flaw size variation results in different Weibull modulus; both the residual stress and Weibull modulus of zirconia before and after grinding are measured in the present study.

2. Experimental

The starting material used in the present study was 3 mol% yttria-doped zirconia (TZ-3Y, Tosoh Co., Tokyo, Japan). Disc-shaped green compacts were first prepared by uniaxial pressing at 13 MPa and then pressureless sintered at 1550 °C in air for 1 h. The heating rate and cooling rate were 5 °C/min. The dimensions of the as-sintered specimens were 18.2 mm in diameter and 2.5 mm in height.

Abrasive grinding was performed using a surface grinder with a resin bonded 325 grit (44 μm) diamond wheel. The diameter of the wheel was 175 mm. The truing and dressing treatments on

* Corresponding author. Fax: +886 223659800.
E-mail address: tuan@ntu.edu.tw (W.-H. Tuan).

Table 1
Residual stress, biaxial strength, Weibull modulus and phase content of the as-sintered, ground, polished and annealed specimens.

	As-sintered	Ground	Polished	Annealed
Relative density/%	99.4 ± 0.2	99.6 ± 0.2	99.3 ± 0.3	99.4 ± 0.1
Elastic modulus/GPa	213 ± 1	212 ± 1	212 ± 1	210 ± 2
Residual stress/MPa	−32*	−1075	−722	−642
Biaxial strength/MPa	914 ± 34	1104 ± 37	981 ± 35	980 ± 66
Weibull modulus	26	28	30	19
Amount of m-phase/mol%	~1	~3	~1	~0
$I_{(0\ 02)_t}/I_{(2\ 00)_t}$	0.6	1.0	0.6	1.4

* Note: “−” denote compressive stress.

diamond wheel had a dramatic effect on the grinding quality.¹² These treatments were carefully carried out before grinding. A water-based oil emulsion grinding fluid was used for cooling. The specimens were ground at a table speed of 0.26 m/s and a wheel surface speed of 36.7 m/s. The depth of cut was 20 μm/pass. The depth of cut was kept constant until 180 μm in thickness of the specimen was removed. Then the depth of cut was reduced to 5 μm/pass till a further 20 μm in thickness was removed. Some ground discs were treated by annealing in air at 1100 °C for 2 h. The heating rate was 5 °C/min and cooling rate was 1 °C/min. An ultrasonic technique was used to determine the elastic modulus of the specimens. A frequency of 5 MHz was applied; the longitudinal velocity and transverse velocity within the specimens were determined. Some specimens were polished after grinding with silica sol as the polishing agent.

Two X-ray facilities were used in the present study. A synchrotron X-ray source (BL-17B1 workstation, National Synchrotron Radiation Research Center, Hsinchu, Taiwan) was used for phase analysis. The X-ray incident angle was 15°; The corresponding penetration depth was around 5 μm.^{13,14} The scanning rate was 0.3° 2θ/min. The amount of monoclinic phase was estimated by using the relationship proposed by Evans et al.¹⁵ The residual stress in the surface region was measured by using the X-ray $\sin^2 \psi$ technique (D5000, Siemens Co., Germany). The diffraction angle 2θ varied from 144° to 146°. The X-ray incident angle for this facility was 5°; the corresponding X-ray penetration depth was around 2 μm.^{13,14}

The flexural strength was determined by using a biaxial bending technique. A one-ball on three-ball fixture was used. An equivalent diameter of 9.7 mm was under tensile stress during bending. The biaxial test was performed with a universal testing machine (MTS810, MTS Co., USA) at ambient conditions. The loading rate was 0.48 mm/min. Twenty-five discs were used to calculate each Weibull modulus. For microstructure observation, the cross-section of the specimens was obtained by cutting, grinding and polishing. The grain boundaries were revealed by thermal etching at 1400 °C for 0.3 h. The microstructure was observed by using scanning electron microscopy (SEM, XL30, Philip Co., Netherland). The grain size was measured from the SEM micrographs and calculated by using the line intercept technique. More than 300 grains was counted.

In order to investigate the effect of annealing treatment on the size of surface flaws, an artificial surface flaw was introduced at the center of each disc by using Vickers indentation at a load of 300 N. Three sets specimens were prepared: one set

specimens were ground then introduced with the indentation-induced flaw (GI); one set specimens were ground, introduced with the flaw then annealed at 1100 °C for 2 h (GIA); one set specimens were ground, annealed then introduced with the flaw (GAI). Ten specimens were prepared for each set.

3. Results

The relative density of the as-sintered discs is 99.4 ± 0.2%. The elastic moduli of the as-sintered, ground, polished and annealed specimens are very close to each other, Table 1. A typical SEM micrograph for the as-sintered specimens is shown in Fig. 1. The average grain size of the as-sintered specimen is 0.72 μm.

Fig. 2 shows the XRD patterns of the as-sintered, ground, polished and annealed specimens. Since the intensity of the synchrotron X-ray is very high, an amount as low as 1 mol% can be detected. A very small amount of monoclinic (m) phase is detected in the as-sintered specimen, Table 1. The amount of m-phase increases to 3 mol% after diamond abrasive grinding. There is a hump at the left shoulder of the tetragonal (t) (1 1 1) peak, as indicated with an arrow. The hump is no longer found after polishing and annealing. The amount of m phase is decreased after the polishing and annealing. The intensity ratio of (0 0 2)_t over (2 0 0)_t peaks is increased after grinding, then decreased after polishing, Table 1. The Weibull statistics for the strength of as-sintered, ground, polished and annealed specimens are shown in Fig. 3. The corresponding values of the

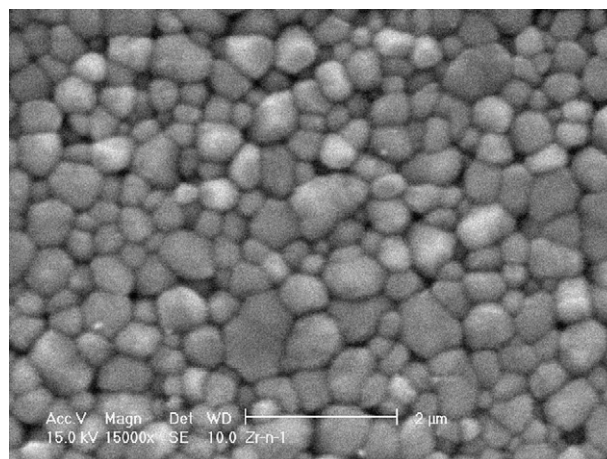


Fig. 1. SEM micrograph of the sintered specimen.

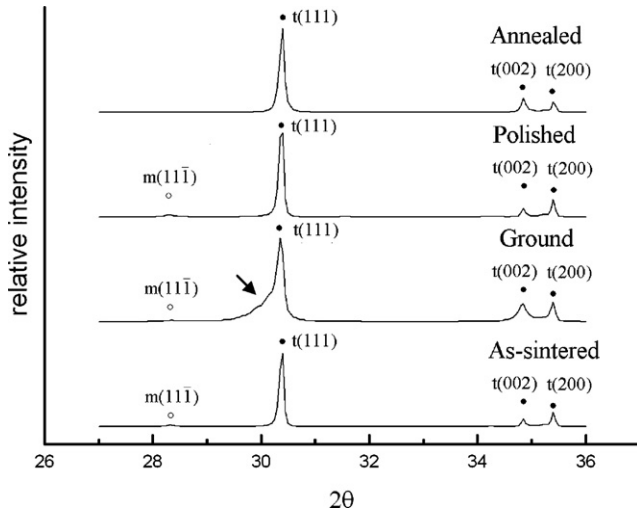


Fig. 2. XRD patterns for the as-sintered, ground, polished and annealed specimens.

Weibull modulus are shown in Table 1. The Weibull modulus of the annealed specimen is lower than that of the as-sintered, ground and annealed specimens.

The grain size changes little after annealing, Table 1. The change of Weibull modulus reflects the change of flaw size variation. In order to estimate the effect of the annealing treatment on the size of flaws, an artificial flaw is introduced into the surface region by using Vickers indentation at a load of 300 N. Fig. 4 shows a typical surface flaw induced by the indentation. The surface flaw exhibits a Palmqvist-type crack which is a typical indentation-induced flaw for Y-TZP.¹⁶ The indentation-induced crack penetrates into the surface by a depth around 400 μm . The average strength of the GI specimens is then reduced from 1075 to 363 MPa, see Tables 1 and 2. The average strength of GIA specimens is higher than that of GI specimens. It indicates that the artificial flaw is reduced in size after the annealing treatment. As the specimens are first heat treated at 1100 $^{\circ}\text{C}$ for 2 h then introduced with the surface flaw, the strength of the GAI specimens is very close to that of the GI specimens, Table 2.

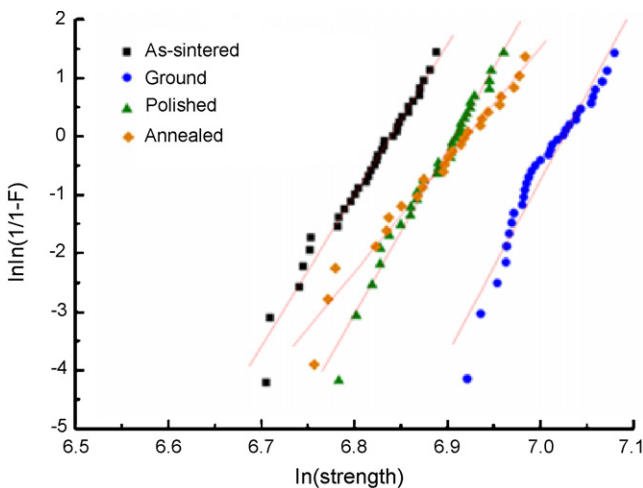


Fig. 3. Weibull statistics for the strength of as-sintered, ground, polished and annealed specimens.

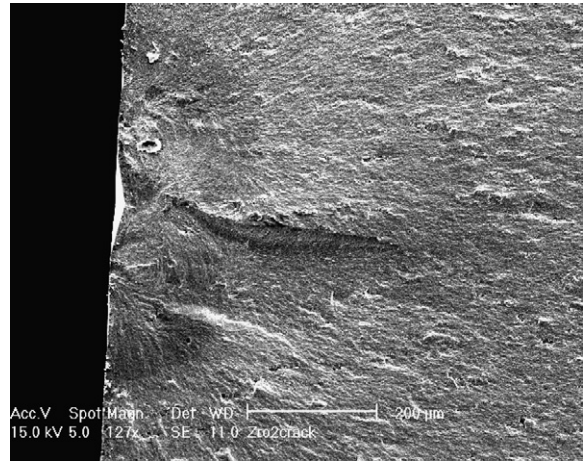


Fig. 4. A typical surface flaw produced by Vickers indentation.

Table 2
Biaxial strength of the discs with the artificial flaws.

	Biaxial strength/MPa
Ground + indented (GI)	363 \pm 19
Ground + indented + annealed (GIA)	451 \pm 33
Ground + annealed + indented (GAI)	351 \pm 31

Note: artificial flaw was generated by Vickers indentation at 300 N.

It suggests that the strength increase after annealing is mainly induced by the crack healing during annealing.

4. Discussion

The values of Weibull modulus obtained in the present study vary in the range of 19–30, which are higher than the reported values (4–10) for rectangular testing bars.¹¹ The abrasive grinding may produce cracks at the edges of specimens. Since the biaxial testing is used for strength measurement, the edges of the specimen disc are outside the tensile stress field. The edge cracks thus have little influence on the biaxial strength. The comparison on the strength of as-received and ground specimens can then be made. There are 25 specimens used for each line in Fig. 3. The accuracy of Weibull modulus value depends strongly on the number of specimens used. Ritter et al had applied a Monte Carlo method to estimate the accuracy of Weibull modulus as a function of specimen number.¹⁷ The coefficient of variation (standard variation/average value) for the specimen number of 25 is 0.2. It thus indicates that the Weibull modulus of 26, 28, and 30 are very close to each other. The flaw size scatter of as-sintered, ground and polished specimens is more or less the same. It also suggests that the Weibull modulus of the annealed specimens is indeed lower than that of the as-sintered, ground and polished specimens.

The annealing treatment is taken place at elevated temperature. Such heat treatment can induce crack opening¹⁸ and crack healing.¹⁹ As demonstrated in Table 2, a heat treatment at 1100 $^{\circ}\text{C}$ for 2 h can induce crack healing in the zirconia specimens. Assuming that all cracks within the specimens undergo the same amount of crack healing during annealing. For smaller

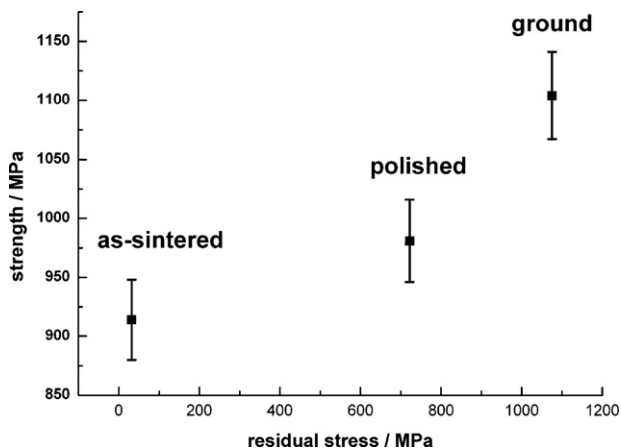


Fig. 5. Strength variation as function of residual stress.

cracks, the crack healing process reduces significantly the size of small crack. For larger cracks, the crack healing may just reduce its size by a very small extent. Though the size of all cracks is decreased, the scatter of flaw size is increased. The Weibull modulus is therefore decreased. However, some residual stress remains after annealing, implying that the annealing temperature is not high enough to remove all the residual stress.

A hump is observed at the left shoulder of the XRD $(1\ 1\ 1)_t$ peak for the ground specimen, Fig. 2. The hump has been related to the formation of orthorhombic or rhombohedral phase^{20,21} or lattice distortion.²² The formation of orthorhombic or rhombohedral phase is induced by the external stress. The lattice distortion is also resulted from the presence of residual stress. Therefore, the presence of the hump at the left shoulder of $(1\ 1\ 1)_t$ peak is a direct evidence for the presence of residual stress. The change of $I_{(002)_t}/I_{(200)_t}$ ratio has been used as an indication for domain re-orientation.²³ It thus suggests that the residual stress is large enough to induce lattice distortion.

The residual stress analysis technique indicates that the grinding process introduces a compressive stress of 1 GPa into the surface region. However, the analysis determines only the stress in a surface region within a depth around 2 μm . The strength of the specimens is increased by only 190 MPa after abrasive grinding. The strength of ceramics is determined by the stress field around the tip of critical flaw. As long as the tip of critical flaw is located under the surface, the strength increase is lower than the surface compressive stress. The Weibull modulus for the as-sintered, ground and polished specimens are very close to each other, suggesting that the flaw size distribution is very similar. The contribution of residual stress on the strength of zirconia can therefore be estimated by using only the strength of as-sintered, ground and polished specimens. Fig. 5 shows the strength as a function of residual stress. It demonstrates that the strength of zirconia can be enhanced by introducing residual stress. The diamond abrasive grinding is an effective method to produce residual stress at surface region.

The polishing treatment removes a very small amount of material from the surface. The residual stress is reduced from 1075 to 722 MPa (Table 1). It also confirms that the residual stress is present at a shallow surface region.

5. Conclusions

In the present study, the effect of abrasive grinding on the strength of Y-TZP is investigated. Our results demonstrate that the abrasive grinding is an effective process to introduce a compressive stress into the surface region. However, the grinding conditions have to be carefully controlled to avoid increasing flaw size. The residual compressive stress can be as high as 1000 MPa. The strength of zirconia is consequently increased by nearly 200 MPa. A polishing process can remove partly the residual stress. A post-grinding heat treatment can also release some residual stress; nevertheless, it also reduces the Weibull modulus.

Acknowledgments

The present work was supported by the National Science Council, Taiwan, through contract number of NSC95-2221-E-002-083. The help on the X-ray analysis from Dr. H.Y. Lee of the National Synchrotron Radiation Research Center, Hsinchu, Taiwan, is highly appreciated.

References

- Ruhle, M. and Evans, A. G., High toughness ceramics and ceramic-matrix composites. *Prog. Mater. Sci.*, 1989, **33**, 85–167.
- Hannink, R. H. J., Kelly, P. M. and Muddle, B. C., Transformation toughening in zirconia-containing ceramics. *J. Am. Ceram. Soc.*, 2000, **83**, 461–487.
- Frank, F. C., Lawn, B. R. and Lang, A. R., A study of strains in abraded diamond surfaces. *Proc. R. Soc. Lond., Ser. A*, 1967, **310**, 239–252.
- Bernal, E. and Koepke, B. G., Residual stresses in machined MgO crystals. *J. Am. Ceram. Soc.*, 1973, **56**, 634–639.
- Cook, R. F., Lawn, B. R., Dabbs, T. P. and Chantikul, P., Effect of machining damage on the strength of a glass ceramic. *J. Am. Ceram. Soc.*, 1981, **64**, c-121–c-122.
- Marshall, D. B., Evans, A. G., Khuri-Yakub, B. T., Tien, J. W. and Kino, G. S., The nature of machining damage in brittle materials. *Proc. R. Soc. Lond., Ser. A*, 1983, **385**, 461–475.
- Lange, F. F., James, M. R. and Green, D. J., Determination of residual surface stresses caused by grinding in polycrystalline Al_2O_3 . *J. Am. Ceram. Soc.*, 1983, **66**, c-16–c-17.
- Johnson-Walls, D., Evans, A. G., Marshall, D. B. and James, M. R., Residual stresses in machined ceramics. *J. Am. Ceram. Soc.*, 1986, **69**, 44–47.
- Tuan, W. H. and Kuo, J. C., Contribution of residual stress to the strength of abrasive ground alumina. *J. Eur. Ceram. Soc.*, 1999, **19**, 1593–1597.
- Kosmac, T., Oblak, C., Jevnikar, P., Funduk, N. and Marion, L., The effect of surface grinding and sandblasting on flexural strength and reliability of Y-TZP zirconia ceramic. *Dent. Mater.*, 1999, **15**, 426–433.
- Luthardt, R. G., Holzhueter, M., Sandkuhl, O., Herold, V., Schnapp, J. D., Kuhlisch, E. and Walter, M., Reliability and properties of ground Y-TZP-zirconia ceramics. *J. Dent. Res.*, 2002, **81**, 487–491.
- Tuan, W. H. and Kuo, J. C., Effect of truing of diamond wheel on the strength of alumina after abrasive grinding. *J. Mater. Sci. Lett.*, 1997, **16**, 806–808.
- Toney, M. F., Huang, T. C., Brennan, S. and Rek, Z., X-ray depth profiling of iron oxide thin films. *J. Mater. Res.*, 1988, **3**, 351–356.
- Marra, W.C., Eisenberger, P., and Cho, A., X-ray total-external-reflection-Bragg diffraction: A structural study on the BaAs-Al interface. *J. Appl. Phys.*, 1070, **50**, 6927–6933.
- Evans, P. A., Stevens, R. and Binner, J. G. P., Quantitative X-ray diffraction analysis of polymorphic mixes of pure zirconia. *Br. Ceram. Trans. J.*, 1984, **83**, 39–43.

16. Kailszewski, M. S., Behrens, G., Heuer, A. H., Shaw, M. C., Marshall, D. B., Dransmann, G. W., Steinbrech, R. W., Pajares, A., Guiberteau, F., Cumbreira, F. L. and Dominguez-Rodriguez, A., Indentation studies of Y_2O_3 -stabilized ZrO_2 : I, development of indentation cracks. *J. Am. Ceram. Soc.*, 1994, **77**, 1185–1193.
17. Ritter Jr., J. E., Bandyopadhyay, N. and Jakus, K., Statistical reproducibility of the dynamic and static fatigue experiments. *Am. Ceram. Soc. Bull.*, 1981, **60**, 798–806.
18. Thompson, A. M., Chan, H. M. and Harmer, M. P., Crack healing and stress relaxation in Al_2O_3 . *J. Am. Ceram. Soc.*, 1995, **78**, 567–571.
19. Lange, F. F. and Radford, K. C., Healing of surface cracks in polycrystalline Al_2O_3 . *J. Am. Ceram. Soc.*, 1970, **53**, 420–421.
20. Ruiz, L. and Ready, M. J., Effect of heat treatment on grain size, phase assemblage, and mechanical properties of 3 mol% Y-TZP. *J. Am. Ceram. Soc.*, 1996, **79**, 2331–2340.
21. Kitano, Y., Mori, Y., Ishitani, A. and Masaki, T., Rhombohedral phase in Y_2O_3 -partially-stabilized ZrO_2 . *J. Am. Ceram. Soc.*, 1988, **71**, c34–c36.
22. Kondoh, J., Origin of the hump on the left shoulder of the X-ray diffraction peaks observed in Y_2O_3 -fully and partially stabilized ZrO_2 . *J. Alloys Compd.*, 2004, **375**, 270–282.
23. Virkar, A. V. and Matsumoto, R. L. K., Ferroelastic domain switching as a toughening mechanism in tetragonal zirconia. *J. Am. Ceram. Soc.*, 1986, **69**, c-224–c-226.